



Article

Inhibitory Effects of Dimethylirioresinol, Epimagnolin A, Eudesmin, Fargesin, and Magnolin on Cytochrome P450 Enzyme Activities in Human Liver Microsomes

Ju-Hyun Kim, Soon-Sang Kwon, Hyeon-Uk Jeong and Hye Suk Lee *

Drug Metabolism and Bioanalysis Laboratory, College of Pharmacy, The Catholic University of Korea, Bucheon 420-743, Korea; jhyunkim@catholic.ac.kr (J.-H.K.); zuzutnseo@naver.com (S.-S.K.); wjd1375@hanmail.net (H.-U.J.)

* Correspondence: sianalee@catholic.ac.kr; Tel.: +82-2-2164-4061; Fax: +82-32-342-2013

Academic Editors: David Arráez-Román, Ana Maria Gómez Caravaca and Giovanni Tarantino

Received: 21 March 2017; Accepted: 27 April 2017; Published: 1 May 2017

Abstract: Magnolin, epimagnolin A, dimethylirioresinol, eudesmin, and fargesin are pharmacologically active tetrahydrofurofuranoid lignans found in Flos Magnoliae. The inhibitory potentials of dimethylirioresinol, epimagnolin A, eudesmin, fargesin, and magnolin on eight major human cytochrome P450 (CYP) enzyme activities in human liver microsomes were evaluated using liquid chromatography-tandem mass spectrometry to determine the inhibition mechanisms and inhibition potency. Fargesin inhibited CYP2C9-catalyzed diclofenac 4'-hydroxylation with a K_i value of 16.3 μM , and it exhibited mechanism-based inhibition of CYP2C19-catalyzed [S]-mephenytoin 4'-hydroxylation (K_i , 3.7 μM ; k_{inact} , 0.102 min^{-1}), CYP2C8-catalyzed amodiaquine *N*-deethylation (K_i , 10.7 μM ; k_{inact} , 0.082 min^{-1}), and CYP3A4-catalyzed midazolam 1'-hydroxylation (K_i , 23.0 μM ; k_{inact} , 0.050 min^{-1}) in human liver microsomes. Fargesin negligibly inhibited CYP1A2-catalyzed phenacetin *O*-deethylation, CYP2A6-catalyzed coumarin 7-hydroxylation, CYP2B6-catalyzed bupropion hydroxylation, and CYP2D6-catalyzed bufuralol 1'-hydroxylation at 100 μM in human liver microsomes. Dimethylirioresinol weakly inhibited CYP2C19 and CYP2C8 with IC_{50} values of 55.1 and 85.0 μM , respectively, without inhibition of CYP1A2, CYP2A6, CYP2B6, CYP2C9, CYP2D6, and CYP3A4 activities at 100 μM . Epimagnolin A, eudesmin, and magnolin showed no the reversible and time-dependent inhibition of eight major CYP activities at 100 μM in human liver microsomes. These *in vitro* results suggest that it is necessary to investigate the potentials of *in vivo* fargesin-drug interaction with CYP2C8, CYP2C9, CYP2C19, and CYP3A4 substrates.

Keywords: dimethylirioresinol; epimagnolin A; eudesmin; fargesin; magnolin; human liver microsomes; cytochrome P450 inhibition

1. Introduction

Magnolin, epimagnolin A, dimethylirioresinol, eudesmin, and fargesin (Figure 1) are the pharmacologically active tetrahydrofurofuranoid lignans found in Flos Magnoliae, *Aristolochia elegans* rhizomes, and *Zanthoxylum armatum* DC. [1–5]. Magnolin, epimagnolin A, dimethylirioresinol, eudesmin, and fargesin exhibit various biological activities, including anti-inflammatory activity [6–10], 5-lipoxygenase inhibitory activity [6], antimycobacterial activity [11], and the inhibition of tumor growth and cancer-catalyzed bone destruction [12]. Fargesin exhibits additional biological activities, including β 1-adrenergic receptor antagonistic and cardioprotective effects [13], stimulation of basal glucose uptake and glucose transporter-4 translocation in muscle cells [14], treatment of dyslipidemia and hyperglycemia in high-fat diet-induced obese mice via activation of Akt and 5'-adenosine

monophosphate-activated protein kinase in white adipose tissue [15], and antihypertensive effects in 2K1C hypertensive rats [16]. Magnolin also inhibits cancer cell migration, invasion, and growth [17–19] and ameliorates contrast-induced nephropathy via antioxidation and antiapoptosis in rats [20].

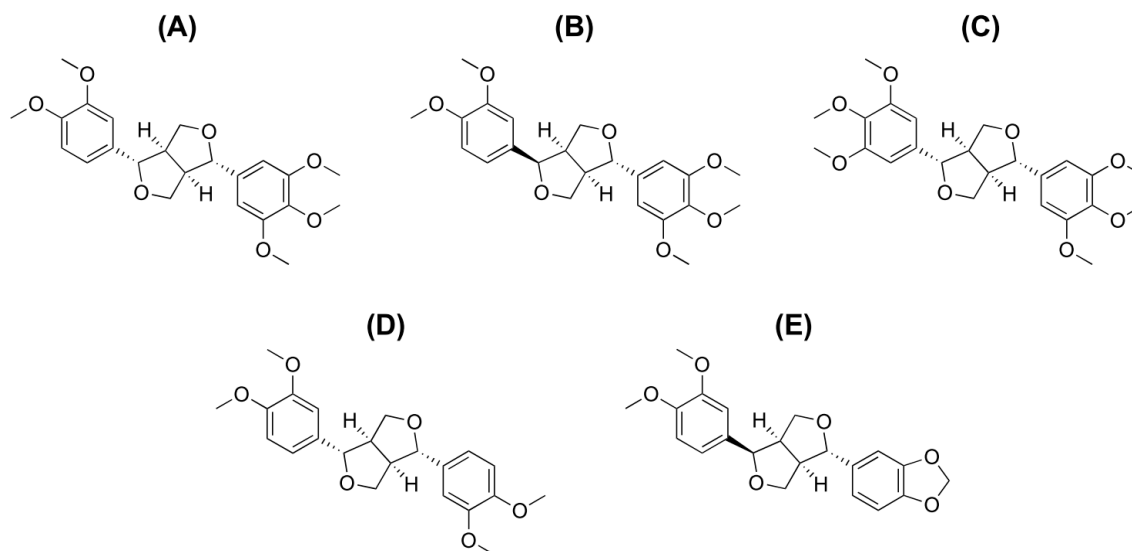


Figure 1. Chemical structures of (A) magnolin; (B) epimagnolin A; (C) dimethyliriioresinol; (D) eudesmin; and (E) fargesin.

Herbal drugs (e.g., *Hypericum perforatum*, *Ginkgo biloba*, *Camellia sinensis*, *Glycyrrhiza glabra*, *Allium sativum*, *Rhizoma Coptidis*, and *Fructus Silybi*) and their constituents cause herb–drug interactions via the induction or inhibition of major drug-metabolizing enzymes, cytochrome P450 (CYP) and result in the toxicity and therapeutic failure of various concomitant drugs [21–31]. For the prediction of herb–drug interaction, it is necessary to investigate the in vitro inhibitory effects of herb drugs and the constituents on major human CYP enzyme activities. In vitro inhibitory effects of the pharmacologically active lignans such as aschantin [32], honokiol [33], machilin A [34], phyllantin, hypophyllantin [35], and podophyllotoxin [36] on CYP enzymes have been reported. However, there are no reports on the in vitro and in vivo inhibitory effects of the bioactive tetrahydrofuranoid lignans such as dimethyliriioresinol, epimagnolin A, eudesmin, fargesin, and magnolin on human CYP enzymes.

In the present study, the in vitro inhibition potency and inhibition mechanisms of dimethyliriioresinol, epimagnolin A, eudesmin, fargesin, and magnolin on 8 major human CYP (CYPs 1A2, 2A6, 2B6, 2C8, 2C9, 2C19, 2D6, and 3A4) activities in pooled human liver microsomes were evaluated to decide the performance of in vivo drug interaction studies of dimethyliriioresinol, epimagnolin A, eudesmin, fargesin, and magnolin.

2. Results

The reversible and time-dependent inhibitory potencies (IC_{50} values) of dimethyliriioresinol, epimagnolin A, eudesmin, fargesin, and magnolin on 8 major human CYP enzymes were investigated in human liver microsomes. Dimethyliriioresinol weakly inhibited CYP2C19-catalyzed [S]-mephenytoin 4'-hydroxylation and CYP2C8-catalyzed amodiaquine N-deethylation with IC_{50} values of 55.1 and 85.0 μ M, respectively, without inhibition of CYP1A2-catalyzed phenacetin O-deethylation, CYP2A6-catalyzed coumarin 7-hydroxylation, CYP2B6-catalyzed bupropion hydroxylation, CYP2C9-catalyzed diclofenac 4'-hydroxylation, CYP2D6-catalyzed bufuralol 1'-hydroxylation, and CYP3A4-catalyzed midazolam 1'-hydroxylation activities at 100 μ M in human liver microsomes (Figure 2).

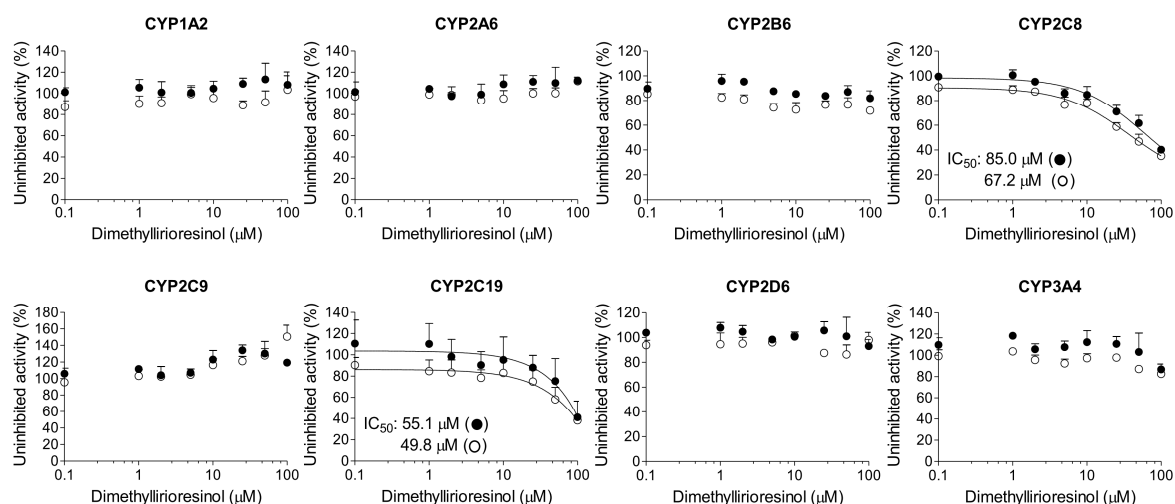


Figure 2. Inhibitory effects of dimethylgliresinol on CYP1A2-mediated phenacetin *O*-deethylation, CYP2A6-mediated coumarin 7-hydroxylation, CYP2B6-mediated bupropion hydroxylation, CYP2C8-mediated amodiaquine *N*-deethylation, CYP2C9-mediated diclofenac 4'-hydroxylation, CYP2C19-mediated [*S*]-mephenytoin 4'-hydroxylation, CYP2D6-mediated bufuralol 1'-hydroxylation, and CYP3A4-mediated midazolam 1'-hydroxylation in pooled human liver microsomes. ○: Pre-incubation of liver microsomes with dimethylgliresinol and reduced β -nicotinamide adenine dinucleotide phosphate (NADPH) for 30 min at 37 °C and ●: No pre-incubation. Data represent the average \pm standard deviation (SD, $n = 3$).

Magnolin, epimagnolin A, and eudesmin negligibly inhibited CYP1A2, CYP2A6, CYP2B6, CYP2C8, CYP2C9, CYP2C19, CYP2D6, and CYP3A4 activities at 100 μ M in human liver microsomes (Figures 3–5).

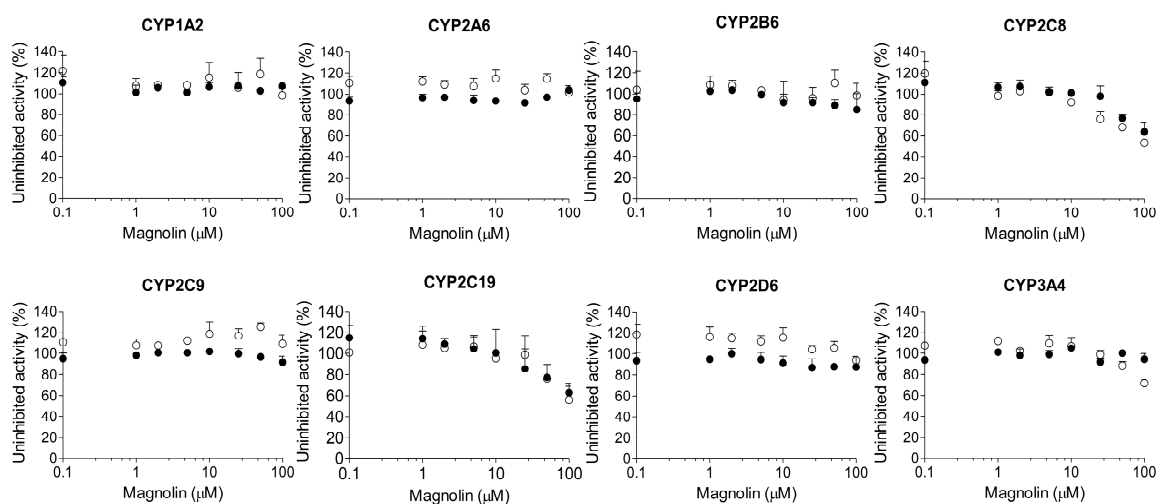


Figure 3. Inhibitory effects of magnolin on CYP1A2-mediated phenacetin *O*-deethylation, CYP2A6-mediated coumarin 7-hydroxylation, CYP2B6-mediated bupropion hydroxylation, CYP2C8-mediated amodiaquine *N*-deethylation, CYP2C9-mediated diclofenac 4'-hydroxylation, CYP2C19-mediated [*S*]-mephenytoin 4'-hydroxylation, CYP2D6-mediated bufuralol 1'-hydroxylation, and CYP3A4-mediated midazolam 1'-hydroxylation in pooled human liver microsomes. ○: Pre-incubation of liver microsomes with magnolin and NADPH for 30 min at 37 °C, ●: No pre-incubation. Data represent the average \pm SD ($n = 3$).

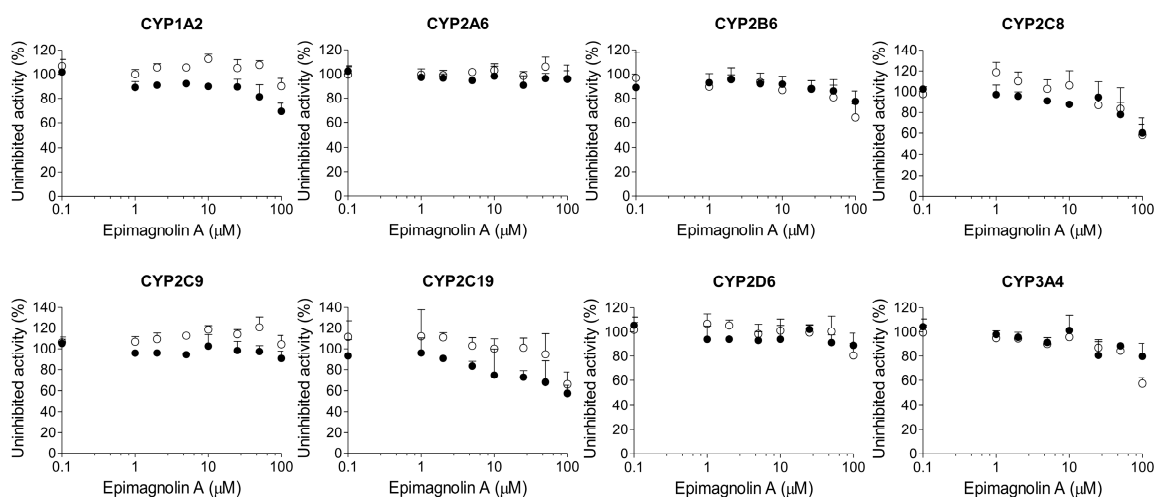


Figure 4. Inhibitory effects of epimagnolin A on CYP1A2-mediated phenacetin *O*-deethylation, CYP2A6-mediated coumarin 7-hydroxylation, CYP2B6-mediated bupropion hydroxylation, CYP2C8-mediated amodiaquine *N*-deethylation, CYP2C9-mediated diclofenac 4'-hydroxylation, CYP2C19-mediated [*S*]-mephenytoin 4'-hydroxylation, CYP2D6-mediated bufuralol 1'-hydroxylation, and CYP3A4-mediated midazolam 1'-hydroxylation in pooled human liver microsomes. ○: Pre-incubation of liver microsomes with epimagnolin A and NADPH for 30 min at 37 °C, ●: No pre-incubation. Data represent the average \pm SD ($n = 3$).

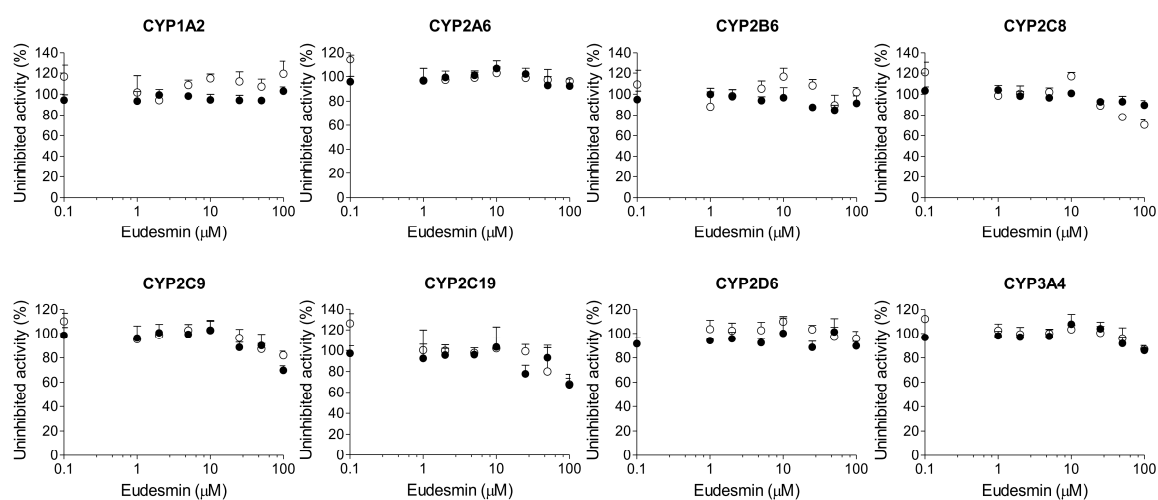


Figure 5. Inhibitory effects of eudesmin on CYP1A2-mediated phenacetin *O*-deethylation, CYP2A6-mediated coumarin 7-hydroxylation, CYP2B6-mediated bupropion hydroxylation, CYP2C8-mediated amodiaquine *N*-deethylation, CYP2C9-mediated diclofenac 4'-hydroxylation, CYP2C19-mediated [*S*]-mephenytoin 4'-hydroxylation, CYP2D6-mediated bufuralol 1'-hydroxylation, and CYP3A4-mediated midazolam 1'-hydroxylation in pooled human liver microsomes. ○: Pre-incubation of liver microsomes with eudesmin and NADPH for 30 min at 37 °C, ●: No pre-incubation. Data represent the average \pm SD ($n = 3$).

Fargesin showed moderate inhibition of CYP2C8-mediated amodiaquine *N*-deethylation, CYP2C9-mediated diclofenac 4'-hydroxylation, and CYP2C19-mediated [*S*]-mephenytoin 4'-hydroxylation with IC_{50} values of 34.9, 30.8, and 30.2 μ M, respectively, in human liver microsomes (Figure 6, Table 1). Fargesin at 100 μ M showed negligible inhibition of CYP1A2, CYP2A6, CYP2B6, CYP2D6, and CYP3A4 activities in human liver microsomes (Figure 6).

A 30-min pre-incubation of dimethyliriioresinol, epimagnolin A, eudesmin, or magnolin with human liver microsomes and reduced β -nicotinamide adenine dinucleotide phosphate (NADPH) did

not cause the IC_{50} value shift of eight CYP enzymes (Figures 2–5), indicating that dimethylirioresinol, magnolin, epimagnolin A, or eudesmin may not be mechanism-based inhibitors. However, 30 min pre-incubation of human liver microsomes with fargesin and NADPH lowered the IC_{50} values of CYP2C8-catalyzed amodiaquine *N*-deethylation, CYP2C19-catalyzed [S]-mephenytoin 4'-hydroxylation, and CYP3A4-catalyzed midazolam 1'-hydroxylation activities by more than 2.5-fold in comparison with the IC_{50} values obtained without pre-incubation (34.9 vs. 4.0 μ M for CYP2C8, 30.2 vs. 1.6 μ M for CYP2C19, and >100 vs. 17.9 μ M for CYP3A4) (Figure 6, Table 1), indicating that fargesin causes potent mechanism-based inhibition of CYP2C8, CYP2C19, and CYP3A4 enzymes in human liver microsomes.

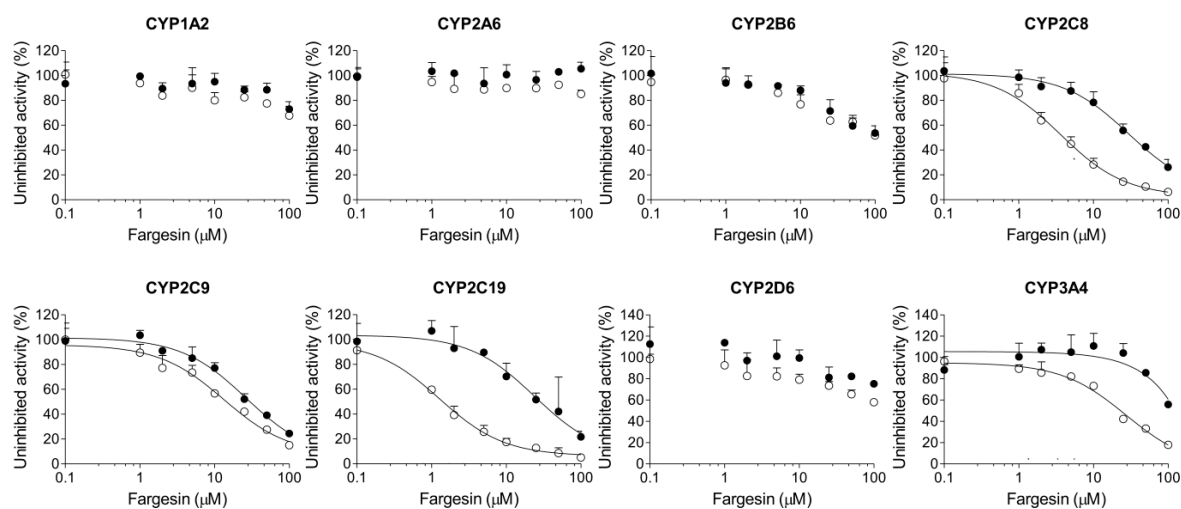


Figure 6. Inhibitory effects of fargesin on CYP1A2-mediated phenacetin *O*-deethylation, CYP2A6-mediated coumarin 7-hydroxylation, CYP2B6-mediated bupropion hydroxylation, CYP2C8-mediated amodiaquine *N*-deethylation, CYP2C9-mediated diclofenac 4'-hydroxylation, CYP2C19-mediated [S]-mephenytoin 4'-hydroxylation, CYP2D6-mediated bufuralol 1'-hydroxylation, and CYP3A4-mediated midazolam 1'-hydroxylation in pooled human liver microsomes. ○: Pre-incubation of liver microsomes with fargesin and NADPH for 30 min at 37 °C, ●: No pre-incubation. Data represent the average \pm SD ($n = 3$).

Table 1. Inhibitory effect of fargesin on eight major CYP enzyme activities in pooled human liver microsomes.

CYP	Enzyme Activities	IC_{50} (μ M)		K_i (μ M)
		No Pre-Incubation	With Pre-Incubation *	(k_{inact} , min^{-1} or Inhibition Mode)
1A2	Phenacetin <i>O</i> -deethylase	>100	>100	-
2A6	Coumarin 7-hydroxylase	>100	>100	-
2B6	Bupropion hydroxylase	>100	>100	-
2C8	Amodiaquine <i>N</i> -deethylase	34.9	4.0	10.7 (k_{inact} : 0.082)
2C9	Diclofenac 4'-hydroxylase	30.8	16.4	16.3 (competitive)
2C19	(S)-Mephenytoin 4'-hydroxylase	30.2	1.6	3.7 (k_{inact} : 0.102)
2D6	Bufuralol 1'-hydroxylase	>100	>100	-
3A4	Midazolam 1'-hydroxylase	>100	17.9	23.0 (k_{inact} : 0.050)

* 30 min pre-incubation of fargesin with microsomes and NADPH before the addition of CYP substrates. The substrate cocktail concentrations for the measurement of the IC_{50} values were as following: 50 μ M phenacetin, 2.5 μ M coumarin, 2.0 μ M amodiaquine, 10 μ M diclofenac, 100 μ M [S]-mephenytoin, 5.0 μ M bufuralol, and 2.5 μ M midazolam. Inhibition of CYP2B6 activity was determined separately using 50 μ M bupropion. The data represent the average of three determinations.

In the study of enzyme inhibition, the inhibitor concentration causing half maximal inactivation (K_i value) and the inhibition mode define the interaction of an inhibitor with a particular enzyme.

Fargesin exhibited competitive inhibition of CYP2C9-catalyzed diclofenac 4-hydroxylation with a K_i value of 16.3 μM (Figure 7, Table 1). Fargesin decreased CYP2C8-catalyzed amodiaquine *N*-deethylation, CYP2C19-catalyzed [S]-mephenytoin 4'-hydroxylation, and CYP3A4-catalyzed midazolam 1'-hydroxylation in pre-incubation time- and concentration-dependent manners in human liver microsomes (Figure 8). The apparent K_i and maximal inactivation rate (k_{inact}) values of fargesin were 10.7 μM and 0.082 min^{-1} for CYP2C8-catalyzed amodiaquine *N*-deethylation, 3.7 μM and 0.102 min^{-1} for CYP2C19-catalyzed [S]-mephenytoin 4'-hydroxylation, and 23.0 μM and 0.050 min^{-1} for CYP3A4-catalyzed midazolam 1'-hydroxylation, respectively, in human liver microsomes (Table 1).

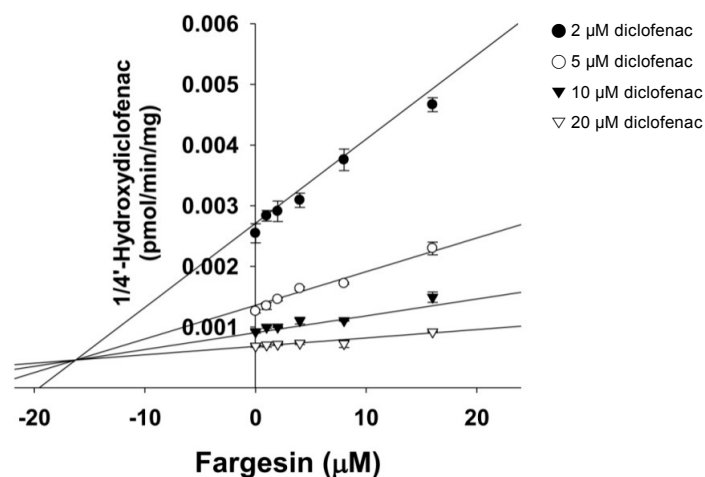


Figure 7. Dixon plot of the inhibitory effects of fargesin on CYP2C9-catalyzed diclofenac 4'-hydroxylation in pooled human liver microsomes. Data represent the average \pm SD ($n = 3$).

3. Discussion

In this study, the *in vitro* inhibitory effects of bioactive tetrahydrofurofuranoid lignans such as dimethyliriioresinol, epimagnolin A, eudesmin, fargesin, and magnolin on 8 major CYP enzymes were, for the first time, evaluated in pooled human liver microsomes. Dimethyliriioresinol exhibited weak inhibition of CYP2C8 and CYP2C19 activities without inhibition of CYP1A2, CYP2A6, CYP2B6, CYP2C9, CYP2D6, and CYP3A4 in human liver microsomes (Figure 2). Magnolin, epimagnolin A, and eudesmin showed no the reversible and time-dependent inhibition of CYP1A2, CYP2A6, CYP2B6, CYP2C8, CYP2C9, CYP2C19, CYP2D6, and CYP3A4 activities at 100 μM in human liver microsomes (Figures 3–5). These results indicate that dimethyliriioresinol, epimagnolin A, eudesmin, and magnolin without a methylenedioxy ring in the chemical structure may not be CYP inhibitors in human liver microsomes. However, fargesin containing a methylenedioxyphenyl moiety in the chemical structure showed moderate reversible inhibition of CYP2C8, CYP2C9, and CYP2C19 activities (IC_{50} values of 34.9, 30.8, and 30.2 μM , respectively) and the potent time-dependent inhibition of CYP2C19, CYP2C8, and CYP3A4 activities (IC_{50} values of 1.6, 4.0, and 17.9 μM , respectively) in human liver microsomes. Aschantin, a chemical derivative of fargesin, with a methylenedioxyphenyl moiety also exhibited the reversible and time-dependent inhibition of CYP2C8, CYP2C9, CYP2C19, and CYP3A4 activities in human liver microsomes [32]. These results indicate that CYP inhibitory capacity of tetrahydrofurofuranoid lignans depends on the presence of a methylenedioxyphenyl moiety. Other methylenedioxyphenyl compounds such as myristicin and podophyllotoxin exhibited mechanism-based inactivation of CYP1A2 and CYP3A4, respectively, in human liver microsomes [36,37].

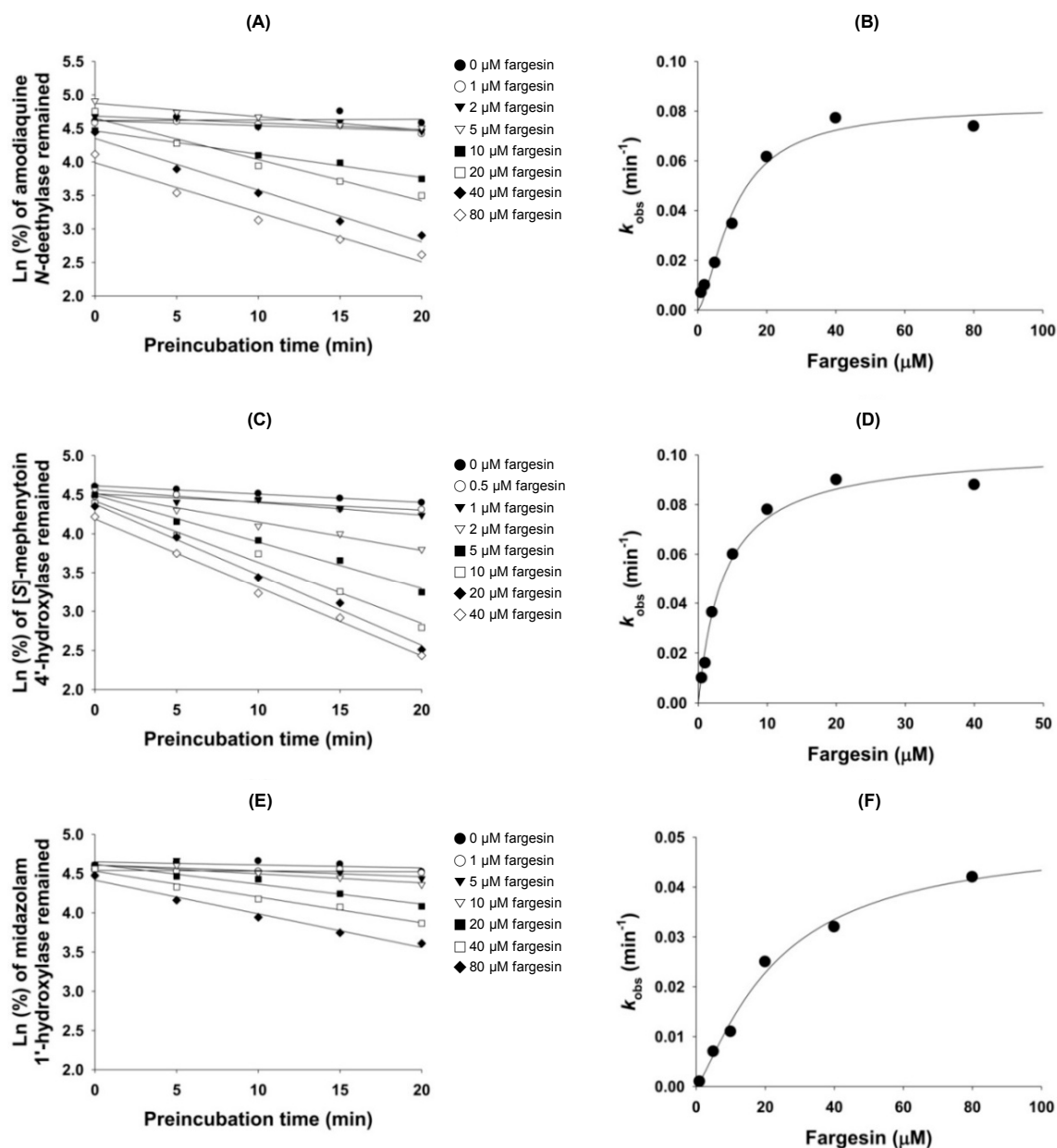


Figure 8. (A) Inactivation of human liver microsomal formation of *N*-desethylamodiaquine from amodiaquine by various fargesin concentrations; (B) The relationship between the observed k (k_{obs}) and fargesin concentration for the estimation of the K_i and k_{inact} values of CYP2C8-catalyzed amodiaquine *N*-deethylation; (C) Inactivation of human liver microsomal formation of 4'-hydroxy-[S]-mephenytoin from [S]-mephenytoin by various fargesin concentrations; (D) The relationship between k_{obs} and fargesin concentration for the estimation of the K_i and k_{inact} values of CYP2C19-catalyzed [S]-mephenytoin 4'-hydroxylation; (E) Inactivation of human liver microsomal formation of 1'-hydroxymidazolam from midazolam by various fargesin concentrations; and (F) The relationship between the k_{obs} and fargesin concentration for the estimation of the K_i and k_{inact} values of CYP3A4-catalyzed midazolam 1'-hydroxylation.

Fargesin exhibited competitive inhibition of CYP2C9-catalyzed diclofenac 4'-hydroxylation (K_i , 16.3 μM), but aschantin showed mechanism-based inhibition of CYP2C9 (K_i , 3.7 μM ; k_{inact} , 0.044 min^{-1}) [32]. Other pharmacologically active lignans such as honokiol, deoxy podophyllotoxin, and podophyllotoxin potently inhibited CYP2C9 activity with K_i values of 0.54, 3.5, and 2.0 μM , respectively [33,36,38].

Fargesin showed mechanism-based inhibition of CYP2C8-catalyzed amodiaquine *N*-deethylation, CYP2C19-catalyzed [*S*]-mephenytoin 4'-hydroxylation, and CYP3A4-catalyzed midazolam 1'-hydroxylation in pooled human liver microsomes (Figure 8). The inactivation potency (k_{inact}/K_i ratio) of fargesin against CYP2C8 ($7.66 \text{ min}^{-1} \text{ nM}^{-1}$) was comparable to that of aschantin ($k_{\text{inact}}/K_i = 5.49 \text{ min}^{-1} \text{ nM}^{-1}$) [32], but was higher than those of mechanism-based CYP2C8 inhibitors such as amiodarone ($0.57 \text{ min}^{-1} \text{ nM}^{-1}$), phenelzine ($3.17 \text{ min}^{-1} \text{ nM}^{-1}$) [39], and gemfibrozil ($1.24 \text{ min}^{-1} \text{ nM}^{-1}$) [40] in human liver microsomes, indicating that fargesin may be a potent mechanism-based inhibitor of CYP2C8.

The inactivation potency (k_{inact}/K_i ratio) of fargesin against CYP2C19 ($27.57 \text{ min}^{-1} \text{ nM}^{-1}$) was higher than those of drugs identified as mechanism-based inhibitors of CYP2C19 such as aschantin ($8.28 \text{ min}^{-1} \text{ nM}^{-1}$), clopidogrel ($3.90 \text{ min}^{-1} \text{ nM}^{-1}$), and fluoxetine ($2.14 \text{ min}^{-1} \text{ nM}^{-1}$), but was comparable to that of ticlopidine ($22.3 \text{ min}^{-1} \text{ nM}^{-1}$) [41] in human liver microsomes.

The CYP3A4 inactivation potency (k_{inact}/K_i ratio) of fargesin ($2.17 \text{ min}^{-1} \text{ nM}^{-1}$) was comparable with those reported for some phytochemicals identified as mechanism-based inhibitors of CYP3A4 including aschantin ($4.92 \text{ min}^{-1} \text{ nM}^{-1}$) [32], bergamottin ($2 \text{ min}^{-1} \text{ nM}^{-1}$) [42], and rutaecarpine ($3.59 \text{ min}^{-1} \text{ nM}^{-1}$) [43], but much lower than those reported for podophyllotoxin ($13.63 \text{ min}^{-1} \text{ nM}^{-1}$) [36], phyllanthin ($131.88 \text{ min}^{-1} \text{ nM}^{-1}$) and hypophyllanthin ($83.21 \text{ min}^{-1} \text{ nM}^{-1}$) [35] in human liver microsomes. The k_{inact}/K_i ratio of fargesin against CYP3A4 was comparable to those of therapeutic drugs known as mechanism-based CYP3A4 inhibitors such as clarithromycin ($1\text{--}13 \text{ min}^{-1} \text{ nM}^{-1}$), erythromycin ($3\text{--}9 \text{ min}^{-1} \text{ nM}^{-1}$), amiodarone ($4.5 \text{ min}^{-1} \text{ nM}^{-1}$), and fluoxetine ($3.2 \text{ min}^{-1} \text{ nM}^{-1}$) in human liver microsomes [43].

4. Materials and Methods

4.1. Materials and Reagents

Epimagnolin A, eudesmin, fargesin, and magnolin were obtained from PhytoLab GmbH & Co. (Vestenbergsgreuth, Germany). Dimethylirioresinol was a gift from Natural Medicine Research Center in Korea Research Institute of Biology and Biotechnology (Ochang, Korea). Bufuralol hydrochloride, 1'-hydroxybufuralol maleate, *d*₉-1'-hydroxybufuralol maleate, bupropion, hydroxybupropion, 4'-hydroxydiclofenac, 1'-hydroxymidazolam, 4'-hydroxymephenytoin, [*S*]-mephenytoin, and pooled human liver microsomes (catalog number 452161) were purchased from Corning Life Sciences (Woburn, MA, USA). Amodiaquine hydrochloride, *N*-desethylamodiaquine dihydrochloride, acetaminophen, coumarin, 7-hydroxycoumarin, diclofenac sodium, midazolam, phenacetin, and NADPH were obtained from Sigma-Aldrich (St. Louis, MO, USA). ¹³C₂, ¹⁵N-acetaminophen was obtained from Toronto Research Chemicals (Toronto, ON, Canada). Methanol, acetonitrile, and water (liquid chromatography-mass spectrometry [LC-MS] grade) were purchased from Fischer Scientific (Fair Lawn, NJ, USA). All other chemicals were of the highest quality available.

4.2. Inhibitory Effects of Dimethylirioresinol, Epimagnolin A, Eudesmin, Fargesin, and Magnolin on 8 Major CYP Activities in Human Liver Microsomes

The degree of inhibition (IC₅₀ values) of dimethylirioresinol, epimagnolin A, eudesmin, fargesin, and magnolin toward CYP1A2, CYP2A6, CYP2C8, CYP2C9, CYP2C19, CYP2D6, and CYP3A4 activities in pooled human liver microsomes were evaluated following our previous method using CYP cocktail substrates and liquid chromatography-tandem mass spectrometry (LC-MS/MS) [33]. The incubation mixtures were prepared in total volumes of 100 μL as follows: 50 mM potassium phosphate buffer (pH 7.4), 1.0 mM NADPH, 10 mM MgCl₂, pooled human liver microsomes (0.2 mg/mL), various concentrations of dimethylirioresinol, epimagnolin A, eudesmin, fargesin, or magnolin in acetonitrile (final concentrations of 0.1–100 μM, acetonitrile 0.5% (*v/v*)), and a cocktail of seven CYP probe substrates (2.0 μM amodiaquine, 5 μM bufuralol, 2.5 μM coumarin, 10 μM diclofenac, 100 μM [*S*]-mephenytoin, 2.5 μM midazolam, and 50 μM phenacetin, acetonitrile 0.5% (*v/v*)). After 3 min

pre-incubation at 37 °C, the reaction mixtures were incubated for 15 min at 37 °C with the addition of NADPH in a shaking water bath. The reaction was stopped by adding 100 µL of ice-cold methanol containing internal standards (d_9 -1'-hydroxybupropion for 1'-hydroxybupropion, 4'-hydroxydiclofenac, 7-hydroxycoumarin, 1'-hydroxymidazolam, and 4'-hydroxymephenytoin; $^{13}C_2$, ^{15}N -acetaminophen for acetaminophen and *N*-desethylamodiaquine). The mixtures were centrifuged at 13,000× *g* for 4 min at 4 °C. All assays were performed in triplicate and the average values were used for the subsequent calculations. For the measurement of time-dependent inhibition, human liver microsomes were pre-incubated with the various concentrations of dimethylirioresinol, epimagnolin A, eudesmin, fargesin, or magnolin in acetonitrile (0.1–100 µM) and NADPH for 30 min at 37 °C. Then, the reaction mixtures were incubated with addition of the seven-CYP probe substrate cocktail for 15 min at 37 °C. The control reaction was performed by adding acetonitrile instead of the test compounds.

Seven metabolites were simultaneously determined using a tandem mass spectrometer (TSQ Quantum Access; Thermo Scientific, San Jose, CA, USA) equipped with an electrospray ionization (ESI) source coupled to a NANOSPACE SI-2 LC system (Shiseido, Tokyo, Japan). The column and autosampler temperatures were 50 and 6 °C, respectively. The ESI source settings for the ionization of metabolites were as follows: polarity, positive ion mode; capillary voltage, 4200 V; capillary temperature, 330 °C; vaporizer temperature, 350 °C; auxiliary gas pressure, 15 psi; and sheath gas pressure, 35 psi. Selected reaction monitoring (SRM) mode with the molecular ion and the intensive product ion was used for the quantification of each metabolite and internal standard, as follows: 1'-hydroxybupropion, 278.1 > 186.1; *N*-desethylamodiaquine, 328.1 > 283.0; acetaminophen, 152.1 > 110.3; 7-hydroxycoumarin, 163.0 > 107.2; 4'-hydroxymephenytoin, 235.1 > 150.1; 4'-hydroxydiclofenac, 312.0 > 231.1; d_9 -1'-hydroxybupropion, 287.2 > 187.0; and $^{13}C_2$, ^{15}N -acetaminophen, 155.1 > 111.2. Analytical data were processed using Xcalibur™ software (Thermo Scientific, San Jose, CA, USA).

For the evaluation of the inhibitory effects of dimethylirioresinol, epimagnolin A, eudesmin, fargesin, and magnolin on CYP2B6-catalyzed bupropion hydroxylation, each incubation mixture in a total volume of 100 µL contained 50 mM potassium phosphate buffer (pH 7.4), 10 mM MgCl₂, pooled human liver microsomes (0.2 mg/mL), 50 µM bupropion, and various concentrations of dimethylirioresinol, epimagnolin A, eudesmin, fargesin, or magnolin in acetonitrile (0.1–100 µM), according to our previous report [33]. After 3 min pre-incubation at 37 °C, the reaction mixtures were incubated with the addition of NADPH in a shaking water bath for 15 min at 37 °C. The reaction was stopped by adding 100 µL of ice-cold d_9 -1'-hydroxybupropion (internal standard) in methanol. The mixtures were centrifuged at 13,000× *g* for 4 min at 4 °C. All incubations were performed in triplicate, and the average values were used for the subsequent calculations. For the measurement of time-dependent inhibition, pooled human liver microsomes were pre-incubated with various concentrations of dimethylirioresinol, epimagnolin A, eudesmin, fargesin, or magnolin in acetonitrile (0.1–100 µM) and NADPH for 30 min at 37 °C. Then, the reaction mixtures were incubated with the addition of NADPH and bupropion for 15 min at 37 °C. The control reaction was performed by the addition of acetonitrile instead of the test compounds. Hydroxybupropion concentrations were quantified using the LC-MS/MS method described above; the SRM transitions for hydroxybupropion and d_9 -1'-hydroxybupropion were 256.1 > 238.0 and 287.2 > 187.0, respectively.

4.3. Kinetic Analysis of CYP2C9 Inhibition by Fargesin

To determine the K_i values and inhibition mode of fargesin for CYP2C9, various concentrations of fargesin (0–16 µM) and diclofenac (2–20 µM) were incubated with human liver microsomes (0.1 mg/mL), 10 mM MgCl₂, 1 mM NADPH, 50 mM potassium phosphate buffer (pH 7.4) in a total volume of 100 µL for 10 min at 37 °C. The reaction was stopped by adding 100 µL of ice-cold d_9 -1'-hydroxybupropion in methanol (10 ng/mL), and the mixtures were centrifuged at 13,000× *g* for 4 min. 50 µL of the supernatant was diluted with 50 µL of water, and aliquots (5 µL) were analyzed by LC-MS/MS.

4.4. Mechanism-Based Inhibition of CYP2C8, CYP2C19, and CYP3A4 Activities by Fargesin

The mechanism-based inhibition potency of fargesin against human liver microsomal CYP2C8, CYP2C19, and CYP3A4 activities was evaluated. Human liver microsomes (1 mg/mL) were pre-incubated with various concentrations of fargesin and NADPH in 50 mM potassium phosphate buffer (pH 7.4). Aliquots (10 μ L) of the pre-incubation mixtures were collected at 5, 10, 15, and 20 min after the pre-incubation and transferred to new tubes containing CYP substrates (2 μ M amodiaquine for CYP2C8, 100 μ M [S]-mephenytoin for CYP2C19, or 2 μ M midazolam for CYP3A4), 10 mM $MgCl_2$, 1 mM NADPH, and 50 mM potassium phosphate buffer (pH 7.4) in 90 μ L reaction mixtures. The incubation was proceeded for 10 min and stopped by adding 100 μ L of ice-cold *d*₉-1'-hydroxybufuralol in methanol. The mixtures were centrifuged at 13,000 \times g for 4 min at 4 °C, and 50 μ L of each supernatant was diluted with 50 μ L of water. Aliquots (5 μ L) were analyzed by LC-MS/MS, as described above.

4.5. Data Analysis

The IC_{50} values were calculated using SigmaPlot ver. 11.0 (Systat Software, Inc., San Jose, CA, USA). K_i , k_{inact} , and the inhibition mode were determined using Enzyme Kinetics ver. 1.1 (Systat Software, Inc.).

5. Conclusions

Fargesin competitively inhibited CYP2C9-catalyzed diclofenac 4'-hydroxylation with K_i value of 16.3 μ M and exhibited the mechanism-based inhibition of CYP2C19-catalyzed [S]-mephenytoin 4'-hydroxylation, CYP2C8-catalyzed amodiaquine *N*-deethylation, and CYP3A4-catalyzed midazolam 1'-hydroxylation with K_i values of 3.7, 10.7, and 23.0 μ M, respectively, in human liver microsomes. Fargesin negligibly inhibited CYP1A2, CYP2A6, CYP2B6, and CYP2D6 activities at 100 μ M. Dimethylirioresinol weakly inhibited CYP2C19 and CYP2C8 with IC_{50} values of 55.1 and 85.0 μ M, respectively, without inhibition of CYP1A2, CYP2A6, CYP2B6, CYP2C9, CYP2D6, and CYP3A4 activities at 100 μ M in human liver microsomes. Epimagnolin A, eudesmin, and magnolin showed no reversible or time-dependent inhibition of 8 major CYP activities at 100 μ M in human liver microsomes. These in vitro results suggest that it is necessary to investigate fargesin-induced in vivo drug interaction studies via the inhibition of CYP2C8, CYP2C9, CYP2C19, and CYP3A4 activities.

Acknowledgments: This work was supported by the Korea Health Technology R&D Project through the Korea Health Industry Development Institute (KHIDI), funded by the Ministry of Health & Welfare, Republic of Korea (HI12C1852) and the National Research Foundation of Korea (NRF) grant, funded by the Korea government (MSIP) (NRF-2014R1A2A2A01002582).

Author Contributions: Ju-Hyun Kim was responsible for the study design, data analysis, experiments, and writing of the manuscript. Soon-Sang Kwon and Hyeon-Uk Jeong performed the experiments and data analysis. Hye Suk Lee was responsible for the study conception and design, data analysis, and writing of the manuscript.

Conflicts of Interest: The authors declare no conflict of interest.

References

1. Zhou, X.; Chen, C.; Ye, X.; Song, F.; Fan, G.; Wu, F. Analysis of lignans in *Magnoliae flos* by turbulent flow chromatography with online solid-phase extraction and high-performance liquid chromatography with tandem mass spectrometry. *J. Sep. Sci.* **2016**, *39*, 1266–1272. [[CrossRef](#)] [[PubMed](#)]
2. Bhatt, V.; Sharma, S.; Kumar, N.; Sharma, U.; Singh, B. Simultaneous quantification and identification of flavonoids, lignans, coumarin and amides in leaves of *Zanthoxylum armatum* using UPLC-DAD-ESI-QTOF-MS/MS. *J. Pharm. Biomed. Anal.* **2017**, *132*, 46–55. [[CrossRef](#)] [[PubMed](#)]
3. Kumar, V.; Kumar, S.; Singh, B.; Kumar, N. Quantitative and structural analysis of amides and lignans in *Zanthoxylum armatum* by UPLC-DAD-ESI-QTOF-MS/MS. *J. Pharm. Biomed. Anal.* **2014**, *94*, 23–29. [[CrossRef](#)] [[PubMed](#)]

4. Guo, T.; Su, D.; Huang, Y.; Wang, Y.; Li, Y.-H. Ultrasound-assisted aqueous two-phase system for extraction and enrichment of *Zanthoxylum armatum* lignans. *Molecules* **2015**, *20*, 15273–15286. [[CrossRef](#)] [[PubMed](#)]
5. Guo, T.; Deng, Y.X.; Xie, H.; Yao, C.Y.; Cai, C.C.; Pan, S.L.; Wang, Y.L. Antinociceptive and anti-inflammatory activities of ethyl acetate fraction from *Zanthoxylum armatum* in mice. *Fitoterapia* **2011**, *82*, 347–351. [[CrossRef](#)] [[PubMed](#)]
6. Lim, H.; Son, K.H.; Bae, K.H.; Hung, T.M.; Kim, Y.S.; Kim, H.P. 5-Lipoxygenase-inhibitory constituents from *Schizandra fructus* and *Magnolia flos*. *Phytother. Res.* **2009**, *23*, 1489–1492. [[CrossRef](#)] [[PubMed](#)]
7. Baek, J.A.; Lee, Y.D.; Lee, C.B.; Go, H.K.; Kim, J.P.; Seo, J.J.; Rhee, Y.K.; Kim, A.M.; Na, D.J. Extracts of *Magnoliae flos* inhibit inducible nitric oxide synthase via ERK in human respiratory epithelial cells. *Nitric Oxide* **2009**, *20*, 122–128. [[CrossRef](#)] [[PubMed](#)]
8. Kim, J.S.; Kim, J.Y.; Lee, H.J.; Lim, H.J.; Lee, D.Y.; Kim, D.H.; Ryu, J.H. Suppression of inducible nitric oxide synthase expression by furfuran lignans from flower buds of *Magnolia fargesii* in BV-2 microglial cells. *Phytother. Res.* **2010**, *24*, 748–753. [[CrossRef](#)] [[PubMed](#)]
9. Shen, Y.; Li, C.G.; Zhou, S.F.; Pang, E.C.; Story, D.F.; Xue, C.C. Chemistry and bioactivity of *Flos Magnoliae*, a Chinese herb for rhinitis and sinusitis. *Curr. Med. Chem.* **2008**, *15*, 1616–1627. [[CrossRef](#)] [[PubMed](#)]
10. Pham, T.H.; Kim, M.S.; Le, M.Q.; Song, Y.S.; Bak, Y.; Ryu, H.W.; Oh, S.R.; Yoon, D.Y. Fargesin exerts anti-inflammatory effects in THP-1 monocytes by suppressing PKC-dependent AP-1 and NF- κ B signaling. *Phytomedicine* **2017**, *24*, 96–103. [[CrossRef](#)] [[PubMed](#)]
11. Jimenez-Arellanes, A.; Leon-Diaz, R.; Meckes, M.; Tapia, A.; Molina-Salinas, G.M.; Luna-Herrera, J.; Yepez-Mulia, L. Antiprotozoal and antimycobacterial activities of pure compounds from *Aristolochia elegans* rhizomes. *Evid.-Based Complement. Altern. Med.* **2012**, *2012*, 593403. [[CrossRef](#)] [[PubMed](#)]
12. Jun, A.Y.; Kim, H.J.; Park, K.K.; Son, K.H.; Lee, D.H.; Woo, M.H.; Chung, W.Y. Tetrahydrofuran-type lignans inhibit breast cancer-mediated bone destruction by blocking the vicious cycle between cancer cells, osteoblasts and osteoclasts. *Investig. New Drugs* **2014**, *32*, 1–13. [[CrossRef](#)] [[PubMed](#)]
13. Wang, X.; Cheng, Y.; Xue, H.; Yue, Y.; Zhang, W.; Li, X. Fargesin as a potential β 1 adrenergic receptor antagonist protects the hearts against ischemia/reperfusion injury in rats via attenuating oxidative stress and apoptosis. *Fitoterapia* **2015**, *105*, 16–25. [[CrossRef](#)] [[PubMed](#)]
14. Choi, S.S.; Cha, B.Y.; Choi, B.K.; Lee, Y.S.; Yonezawa, T.; Teruya, T.; Nagai, K.; Woo, J.T. Fargesin, a component of *Flos Magnoliae*, stimulates glucose uptake in L6 myotubes. *J. Nat. Med.* **2013**, *67*, 320–326. [[CrossRef](#)] [[PubMed](#)]
15. Lee, Y.S.; Cha, B.Y.; Choi, S.S.; Harada, Y.; Choi, B.K.; Yonezawa, T.; Teruya, T.; Nagai, K.; Woo, J.T. Fargesin improves lipid and glucose metabolism in 3T3-L1 adipocytes and high-fat diet-induced obese mice. *Biofactors* **2012**, *38*, 300–308. [[CrossRef](#)] [[PubMed](#)]
16. Sha, S.; Xu, D.; Wang, Y.; Zhao, W.; Li, X. Antihypertensive effects of fargesin in vitro and in vivo via attenuating oxidative stress and promoting nitric oxide release. *Can. J. Physiol. Pharmacol.* **2016**, *94*, 900–906. [[CrossRef](#)] [[PubMed](#)]
17. Lee, C.-J.; Lee, M.-H.; Yoo, S.-M.; Choi, K.-I.; Song, J.-H.; Jang, J.-H.; Oh, S.-R.; Ryu, H.-W.; Lee, H.-S.; Surh, Y.-J.; et al. Magnolin inhibits cell migration and invasion by targeting the ERKs/RSK2 signaling pathway. *BMC Cancer* **2015**, *15*, 576. [[CrossRef](#)] [[PubMed](#)]
18. Lee, C.J.; Lee, H.S.; Ryu, H.W.; Lee, M.H.; Lee, J.Y.; Li, Y.; Dong, Z.; Lee, H.K.; Oh, S.R.; Cho, Y.Y. Targeting of magnolin on ERKs inhibits Ras/ERKs/RSK2-signaling-mediated neoplastic cell transformation. *Carcinogenesis* **2014**, *35*, 432–441. [[CrossRef](#)] [[PubMed](#)]
19. Huang, Y.; Zou, X.; Zhang, X.; Wang, F.; Zhu, W.; Zhang, G.; Xiao, J.; Chen, M. Magnolin inhibits prostate cancer cell growth in vitro and in vivo. *Biomed. Pharmacother.* **2017**, *87*, 714–720. [[CrossRef](#)] [[PubMed](#)]
20. Wang, F.; Zhang, G.; Zhou, Y.; Gui, D.; Li, J.; Xing, T.; Wang, N. Magnolin protects against contrast-induced nephropathy in rats via antioxidation and antiapoptosis. *Oxid. Med. Cell. Longev.* **2014**, *2014*, 203458. [[CrossRef](#)] [[PubMed](#)]
21. Na, D.H.; Ji, H.Y.; Park, E.J.; Kim, M.S.; Liu, K.H.; Lee, H.S. Evaluation of metabolism-mediated herb-drug interactions. *Arch. Pharm. Res.* **2011**, *34*, 1829–1842. [[CrossRef](#)] [[PubMed](#)]
22. Liu, M.Z.; Zhang, Y.L.; Zeng, M.Z.; He, F.Z.; Luo, Z.Y.; Luo, J.Q.; Wen, J.G.; Chen, X.P.; Zhou, H.H.; Zhang, W. Pharmacogenomics and herb-drug interactions: Merge of future and tradition. *Evid.-Based Complement. Altern. Med.* **2015**, *2015*, 321091. [[CrossRef](#)] [[PubMed](#)]

23. Ma, B.L.; Ma, Y.M. Pharmacokinetic herb-drug interactions with traditional Chinese medicine: Progress, causes of conflicting results and suggestions for future research. *Drug Metab. Rev.* **2016**, *48*, 1–26. [[CrossRef](#)] [[PubMed](#)]
24. Meng, Q.; Liu, K. Pharmacokinetic interactions between herbal medicines and prescribed drugs: Focus on drug metabolic enzymes and transporters. *Curr. Drug Metab.* **2014**, *15*, 791–807. [[CrossRef](#)] [[PubMed](#)]
25. Brantley, S.J.; Argikar, A.A.; Lin, Y.S.; Nagar, S.; Paine, M.F. Herb–drug interactions: Challenges and opportunities for improved predictions. *Drug Metab. Dispos.* **2014**, *42*, 301–317. [[CrossRef](#)] [[PubMed](#)]
26. Roe, A.L.; Paine, M.F.; Gurley, B.J.; Brouwer, K.R.; Jordan, S.; Griffiths, J.C. Assessing natural product–drug interactions: An end-to-end safety framework. *Regul. Toxicol. Pharmacol.* **2016**, *76*, 1–6. [[CrossRef](#)] [[PubMed](#)]
27. Zuo, Z.; Huang, M.; Kanfer, I.; Chow, M.S.; Cho, W.C. Herb-drug interactions: Systematic review, mechanisms, and therapies. *Evid.-Based Complement. Altern. Med.* **2015**, *2015*, 239150. [[CrossRef](#)] [[PubMed](#)]
28. Russo, E.; Scicchitano, F.; Whalley, B.J.; Mazzitello, C.; Ciriaco, M.; Esposito, S.; Patane, M.; Upton, R.; Pugliese, M.; Chimirri, S.; et al. *Hypericum perforatum*: Pharmacokinetic, mechanism of action, tolerability, and clinical drug–drug interactions. *Phytother. Res.* **2014**, *28*, 643–655. [[CrossRef](#)] [[PubMed](#)]
29. Unger, M. Pharmacokinetic drug interactions involving *Ginkgo biloba*. *Drug Metab. Rev.* **2013**, *45*, 353–385. [[CrossRef](#)] [[PubMed](#)]
30. Wang, X.; Zhang, H.; Chen, L.; Shan, L.; Fan, G.; Gao, X. Liquorice, a unique “guide drug” of traditional Chinese medicine: A review of its role in drug interactions. *J. Ethnopharmacol.* **2013**, *150*, 781–790. [[CrossRef](#)] [[PubMed](#)]
31. Jeong, H.U.; Lee, J.Y.; Kwon, S.S.; Kim, J.H.; Kim, Y.M.; Hong, S.W.; Yeon, S.H.; Lee, S.M.; Cho, Y.Y.; Lee, H.S. Metabolism-mediated drug interaction potential of HS-23, a new herbal drug for the treatment of sepsis in human hepatocytes and liver microsomes. *Arch. Pharm. Res.* **2015**, *38*, 171–177. [[CrossRef](#)] [[PubMed](#)]
32. Kwon, S.S.; Kim, J.H.; Jeong, H.U.; Cho, Y.Y.; Oh, S.R.; Lee, H.S. Inhibitory effects of aschantin on cytochrome P450 and uridine 5′-diphospho-glucuronosyltransferase enzyme activities in human liver microsomes. *Molecules* **2016**, *21*, E554. [[CrossRef](#)] [[PubMed](#)]
33. Jeong, H.U.; Kong, T.Y.; Kwon, S.S.; Hong, S.W.; Yeon, S.H.; Choi, J.H.; Lee, J.Y.; Cho, Y.Y.; Lee, H.S. Effect of honokiol on cytochrome P450 and UDP-glucuronosyltransferase enzyme activities in human liver microsomes. *Molecules* **2013**, *18*, 10681–10693. [[CrossRef](#)] [[PubMed](#)]
34. Kim, S.J.; You, J.; Choi, H.G.; Kim, J.A.; Jee, J.G.; Lee, S. Selective inhibitory effects of machilin A isolated from *Machilus thunbergii* on human cytochrome P450 1A and 2B6. *Phytomedicine* **2015**, *22*, 615–620. [[CrossRef](#)] [[PubMed](#)]
35. Taesotikul, T.; Dumrongsakulchai, W.; Wattanachai, N.; Navinpipat, V.; Somanabandhu, A.; Tassaneeyakul, W.; Tassaneeyakul, W. Inhibitory effects of *Phyllanthus amarus* and its major lignans on human microsomal cytochrome P450 activities: Evidence for CYP3A4 mechanism-based inhibition. *Drug Metab. Pharmacokinet.* **2011**, *26*, 154–161. [[CrossRef](#)] [[PubMed](#)]
36. Song, J.H.; Sun, D.X.; Chen, B.; Ji, D.H.; Pu, J.; Xu, J.; Tian, F.D.; Guo, L. Inhibition of CYP3A4 and CYP2C9 by podophyllotoxin: Implication for clinical drug–drug interactions. *J. Biosci.* **2011**, *36*, 879–885. [[CrossRef](#)] [[PubMed](#)]
37. Yang, A.-H.; He, X.; Chen, J.-X.; He, L.-N.; Jin, C.-H.; Wang, L.-L.; Zhang, F.-L.; An, L.-J. Identification and characterization of reactive metabolites in myristicin-mediated mechanism-based inhibition of CYP1A2. *Chem. Biol. Interact.* **2015**, *237*, 133–140. [[CrossRef](#)] [[PubMed](#)]
38. Lee, S.K.; Kim, Y.; Jin, C.; Lee, S.H.; Kang, M.J.; Jeong, T.C.; Jeong, S.Y.; Kim, D.H.; Yoo, H.H. Inhibitory effects of deoxypodophyllotoxin from *Anthriscus sylvestris* on human CYP2C9 and CYP3A4. *Planta Med.* **2010**, *76*, 701–704. [[CrossRef](#)] [[PubMed](#)]
39. Polasek, T.M.; Elliot, D.J.; Lewis, B.C.; Miners, J.O. Mechanism-based inactivation of human cytochrome P4502C8 by drugs in vitro. *J. Pharmacol. Exp. Ther.* **2004**, *311*, 996–1007. [[CrossRef](#)] [[PubMed](#)]
40. Takagi, M.; Sakamoto, M.; Itoh, T.; Fujiwara, R. Underlying mechanism of drug–drug interaction between pioglitazone and gemfibrozil: Gemfibrozil acyl-glucuronide is a mechanism-based inhibitor of CYP2C8. *Drug Metab. Pharmacokinet.* **2015**, *30*, 288–294. [[CrossRef](#)] [[PubMed](#)]
41. Nishiya, Y.; Hagihara, K.; Kurihara, A.; Okudaira, N.; Farid, N.A.; Okazaki, O.; Ikeda, T. Comparison of mechanism-based inhibition of human cytochrome P450 2C19 by ticlopidine, clopidogrel, and prasugrel. *Xenobiotica* **2009**, *39*, 836–843. [[CrossRef](#)] [[PubMed](#)]

42. Tassaneeyakul, W.; Guo, L.Q.; Fukuda, K.; Ohta, T.; Yamazoe, Y. Inhibition selectivity of grapefruit juice components on human cytochromes P450. *Arch. Biochem. Biophys.* **2000**, *378*, 356–363. [[CrossRef](#)] [[PubMed](#)]
43. Iwata, H.; Tezuka, Y.; Kadota, S.; Hiratsuka, A.; Watabe, T. Mechanism-based inactivation of human liver microsomal CYP3A4 by rutaecarpine and limonin from *Evodia* fruit extract. *Drug Metab. Pharmacokinet.* **2005**, *20*, 34–45. [[CrossRef](#)] [[PubMed](#)]



© 2017 by the authors. Licensee MDPI, Basel, Switzerland. This article is an open access article distributed under the terms and conditions of the Creative Commons Attribution (CC BY) license (<http://creativecommons.org/licenses/by/4.0/>).